# Modeling of a LiBr-H2O absorption air conditioner system driven by a solar flat plate collector

Lahcen Bouzyan, Cyril Toublanc, Abdellah Ousegui

# Modeling of a LiBr-$H_2O$ absorption air conditioner system driven by a solar flat plate collector

*Lahcen* Bouzyan[1*], *Cyril* Toublanc[2], and *Abdellah* Ousegui[1]

[1] ERIPA, Faculty of sciences, Moulay Ismail University, B.P. 11201, Meknès, Morocco
[2] ONIRIS, Nantes University, CNRS, GEPEA, UMR 6144, F-44000, Nantes, France

**Abstract.** In regions with hot and mixed climates, the principal energy users in buildings are the systems that provide cooling and air-conditioning. Buildings consume more energy as a result of their reliance on traditional electrically powered systems. Solar energy has emerged as an important alternative for many uses, including cooling and air-conditioning. In this paper, to simulate a solar-assisted single-stage LiBr-$H_2O$ absorption air conditioner system, a mathematical model is presented. The model may simulate either the static or the quasi-static state of the system. The model is constructed using mass and energy balances that are applied to the various components found on the inside of the machine. The experimental data that were acquired for one of the other works in the body of literature are used to validate the model that was developed. In this study, the quantity of energy given by a flat plate solar collector to cool the air in a room in Meknès city on a typical summer day is compared to the cooling load imposed by a cooling fan in the same room. The simulation shows that a flat plate solar collector to power our system can only be used effectively under specific solar irradiance conditions**.**

**Keywords:** Air conditioner, Absorption chiller, Flat plate collector, Lithium bromide, Simulation.

## 1 Introduction

There are two main classes of refrigeration systems: those that consume mechanical energy or its equivalent to operate, i.e., the mechanical refrigeration systems, and those that consume mainly thermal energy, i.e., the thermal refrigeration systems. Conventional vapour compression based refrigeration cycles contribute to the increasing global consumption of limited primary energy. Indeed, the use of fossil energy causes emissions of $CO_2$ into the atmosphere, thus harmful effects on the environment. In addition, the refrigerants used in conventional refrigeration cycles also cause environmental issues: traditional, non-natural

* Corresponding author: bouzyanlahcen@gmail.com

commercial working fluids are causing both depletion of the ozone layer and global warming [1].

The modeling works in the literature, more precisely those that apply a steady-state model, take into account average values of ambient temperature and irradiation. In this work, we study the reliability of such an approach in the real case where $T_{amb}$, $V_w$, and $G_T$, are time depended (transient model). The methodology consists on validating the static model with already existing experimental works and then taking a test case related to one of the climates in Morocco where we compare the static and quasi-static models.

In the present work, a mathematical model for modeling an absorption solar air conditioner with a LiBr-$H_2O$ couple is presented. In the first stage of the process, the MATLAB Simulink software executes the simulation in the static case. The accuracy of the simulation is demonstrated by using experiment data from existing published work. The next step needed is running the simulation using an average summer day as starting point. The goal of this project is to know if a flat plate solar collector could be used to power an air conditioner in very hot conditions.

## 2 Material and methods

### 2.1 The examined system

The fundamental design of a solar thermal absorption air-conditioning system is presented in Figure 1. The most important components of the system are a flat-plate solar collector, a generator, an absorber, a condenser, an evaporator, a heat exchanger, an expansion valve, and a circulating pump.

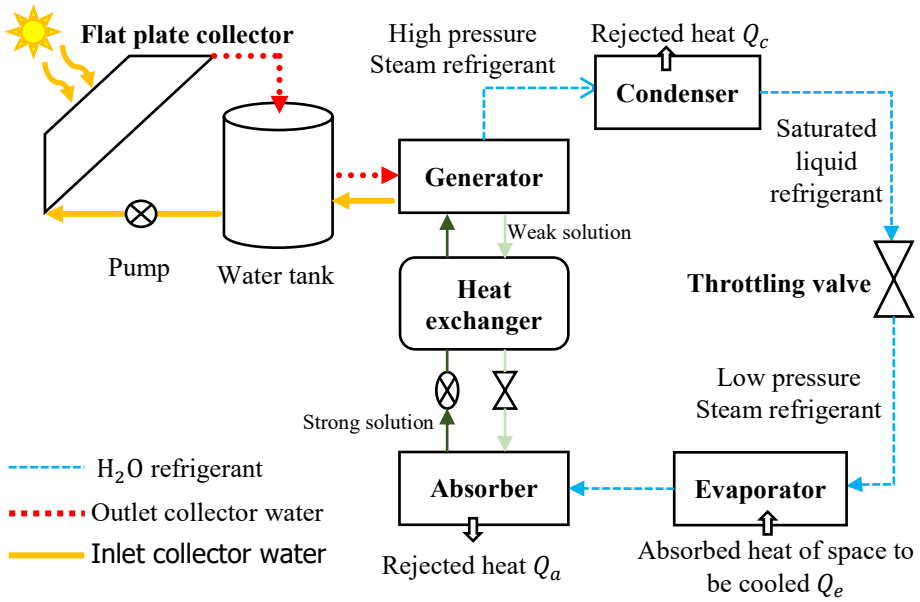


**Fig. 1.** LiBr-$H_2O$ absorption air conditioner powered by a flat plate solar collector.

The basic principle of a single-effect solar air conditioning system with LiBr-$H_2O$ as a working pair can be described as follows:

1. A pump transfers the dilute LiBr solution to the high-pressure region.

2. The thermal collector facilitates the heating of the mixture within the generator. The process allows the desorption of the solution by removing the refrigerant ($H_2O$) from the absorbent (LiBr solution).
3. The refrigerant vapors are directed through the conventional sequence of a condenser, a throttling valve, and an evaporator. The process of cooling is achieved through the evaporation of the refrigerant within the low-pressure evaporator.
4. The rich LiBr solution is returned to the absorber through a throttling valve.
5. The refrigerant vapors are absorbed by the rich solution in the absorber. Then, the cycle has the potential to start anew.

## 2.2 The mathematical model

### *2.2.1 Modeling the flat plate solar collector*

The flat plate collector (FPC) is the type of solar collector that is being considered. This section presents the fundamental equations that describe the thermal behavior of the system. The solar irradiance received by the outer surface of the thermal panel ($Q_{sol}$) is calculated as following [2]:

$$Q_{sol} = A_c G_T \tag{1}$$

Using the energy balance for the fluid volume, ($Q_u$) is given by [3]:

$$Q_u = m_{col}.c_p.\left(T_{col,out} - T_{col,in}\right) \tag{2}$$

The collector's thermal efficiency ($\eta_{th}$) is defined as [3]:

$$\eta_{th} = \frac{Q_u}{Q_{sol}} \tag{3}$$

The mean plate temperature [4]:

$$T_{pm} = T_{col,in} + \frac{Q_u}{F_R.A_c.U_L}.(1 - F_R) \tag{4}$$

The mean fluid temperature [4]:

$$T_{fm} = T_{col,in} + \frac{Q_u}{F_R.A_c.U_L}.(1 - F'') \tag{5}$$

The outlet collector temperature [4]:

$$T_{col,out} = 2T_{fm} - T_{col,in} \tag{6}$$

### *2.2.2 Absorption air conditioning unit*

This section provides the basic equations that describe solution properties as well as the mass and energy balances for each component within the system [5].

#### *2.2.2.1 Absorber unit*

The solution concentration at the outlet to the heat exchanger:

$$X_{a,hex} = \frac{49.04 + 1.125 \times T_a - T_e}{134.65 + 0.47 \times T_a} \tag{7}$$

The mass flow rate of the strong solution:

$$M_{str} = M_r \times \left(\frac{X_{g,hex}}{X_{g,hex} - X_{a,hex}}\right) \quad (8)$$

The mass flow rate of the weak solution:

$$M_{wk} = M_r \times \left(\frac{X_{a,hex}}{X_{g,hex} - X_{a,hex}}\right) \quad (9)$$

The enthalpy of LiBr-$H_2O$ solution of concentration $X$ at temperature $T$, outlet to the heat exchanger unit:

$$H_{a,hex} = H\left(X_{a,hex}, T_a\right) \quad (10)$$

The following correlation can be used to calculate the enthalpy:

$H = (42.81 - 425.92 \times X + 404.67 \times X^2) + (1.01 - 1.23 \times X + 0.48 \times X^2) \times T \times 4.186798$

Absorber thermal capacity:

$$Q_a = \left(M_{wk} \times H_{hex,a}\right) + \left(M_r \times H_{e,abs}\right) - \left(M_{str} \times H_{a,hex}\right) \quad (11)$$

#### *2.2.2.2 Heat exchanger unit*

The temperature of the stream exits the heat exchanger and moves to the absorber unit:

$$T_{hex,a} = T_g - \left(\eta_{HX} \times \left(T_g - T_a\right)\right) \quad (12)$$

The temperature of the stream exits the heat exchanger and moves to the generator unit:

$$T_{hex,g} = T_a + \left(\eta_{hex} \times \left(\frac{X_{a,hex}}{X_{g,hex}}\right) \times \left(\frac{C_p\left(X_{g,hex}\right)}{C_p\left(X_{a,hex}\right)}\right) \times \left(T_g - T_a\right)\right) \quad (13)$$

Where, the specific heat capacity of LiBr-$H_2O$ solution is calculated by the following correlation:

$C_p = (1.01 - 1.23 \times X + 0.48 \times X^2) \times 4.186798$

The enthalpy of LiBr-$H_2O$ solution of concentration $X$ at temperature $T$, outlet to the Absorber unit:

$$H_{hex,a} = H\left(X_{g,hex}, T_{hex,a}\right) \quad (14)$$

The following correlation can be used to calculate the enthalpy:

$H = (42.81 - 425.92 \times X + 404.67 \times X^2) + (1.01 - 1.23 \times X + 0.48 \times X^2) \times T \times 4.186798$

#### *2.2.2.3 Generator unit*

The concentration of the solution at the outlet of the heat exchanger:

$$X_{g,hex} = \frac{49.04 + 1.125 \times T_g - T_c}{134.65 + 0.47 \times T_g} \quad (15)$$

Outlet enthalpy from the generator to the condenser unit:

$$H_{g,cond} = H\left(T_g, T_c\right) \quad (16)$$

The enthalpy is calculated by the following correlation:

$H = (572.8 + 0.46 \times T - 0.043 \times T_s) \times 4.186798$

Generator thermal capacity:

$$Q_g = \left(M_{wk} \times H_{hex,a}\right) + \left(M_r \times H_{g,cond}\right) - \left(M_{str} \times H_{a,hex}\right) \quad (17)$$

Generator efficiency:

$$Eff_g = \frac{T_g - T_c}{T_{col,out} - T_c} \quad (18)$$

#### *2.2.2.4 Condenser unit*

The enthalpy stream that exits from the condenser and goes to the evaporator:

$$H_{c,evp} = (T_c - 25) \times 4.186798 \tag{19}$$

Condenser thermal capacity:

$$Q_c = M_r \times \left(H_{g,cond} - H_{c,evp}\right) \tag{20}$$

#### *2.2.2.5 Evaporator unit*

The enthalpy of saturated water vapor at temperature $T$ from the evaporator to absorber unit:

$$H_{e,abs} = \left(572.8 + (0.417 \times T_e)\right) \times 4.186798 \tag{21}$$

Refrigerant mass flow rate:

$$M_r = \frac{Q_e}{H_{e,abs} - H_{c,evp}} \tag{22}$$

#### *2.2.2.6 Fan unit*

Mean air temperature:

$$T_{ma} = \frac{T_{ai} + T_{ao}}{2} \tag{23}$$

Cooling load:

$$Load = M_{air} C_p(T_{ma}) \times (T_{ai} - T_{ao}) \tag{24}$$

Where:
$C_p = 1.031 + 0.0001369 \times 1.0132 + 0.0001299 \times T$
The COP:

$$COP = \frac{Q_e}{Q_g} \tag{25}$$

The maximum COP:

$$COP_{max} = \frac{(T_e + 273.15) \times \left(T_g - T_a\right)}{\left(T_g + 273.15\right) \times (T_c - T_e)} \tag{26}$$

## 3 Results and discussions

### 3.1 Validation parameters

**Table 1.** The most essential characteristics of the flat plate collector under study [6].

| Parameter | unit | value | description |
|---|---|---|---|
| $A_c$ | $m^2$ | 2.13 | Aperture |
| $L$ | $m$ | 1.905 | Length |

| | | | |
|---|---|---|---|
| $W$ | $m$ | 0.1 | Distance between risers |
| $N_{riser}$ | - | 10 | Number of risers |
| $\varepsilon_p$ | - | 0.15 | Plate emittance |
| $\varepsilon_{gc}$ | - | 0.88 | Cover emittance |
| $\tau$ | - | 0.94 | Cover transmittance |
| $\alpha$ | - | 0.93 | Plate absorbance |
| $D_i$ | $m$ | 0.01 | Riser inner diameter |
| $D_o$ | $m$ | 0.012 | Riser outer diameter |
| $U_b$ | $m^{-2}K^{-1}$ | 0.6 | Back loss coefficient |
| $U_e$ | $m^{-2}K^{-1}$ | 0.4 | Edge loss coefficient |
| $k_p$ | $W.m^{-1}K^{-1}$ | 400 | Plate thermal conductivity |
| $\delta_p$ | $m$ | 0.002 | Plate thickness |
| $\beta$ | ° | 45 | Slope |
| $G_T$ | $W.m^{-2}$ | 500 | Solar irradiation |
| $m_{col}$ | $L.min^{-1}$ | 1.85 | Flow rate |

**Table 2.** The fundamental characteristics of the studied fan cooler.

| **Parameter** | **unit** | **value** | **description** |
|---|---|---|---|
| $T_{ai}$ | ℃ | 35 | Inlet hot air temperature |
| $T_{ao}$ | ℃ | 18 | Outlet cooled air temperature |
| $M_{air}$ | $Kg.min^{-1}$ | 5 | Mass flow rate of the air |

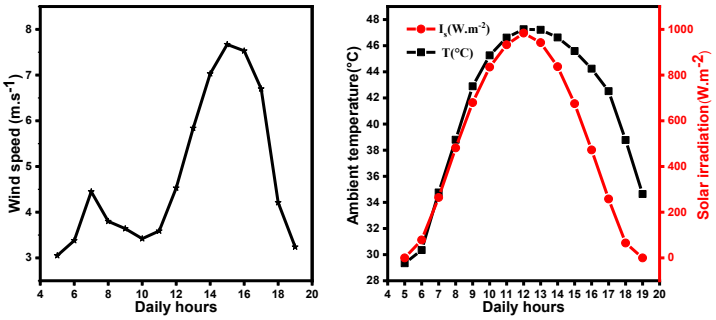


**Fig. 2.** Weather data of a hot summer day in Meknès city [7].

### 3.2 Results and Discussions

All of the results presented in this study are derived from the solution of the equations within the previously developed model. The equations were solved using the MATLAB SIMULINK software. Table 1 provides the specifications of the collector, solar irradiation, and flow rate used in the present analysis.

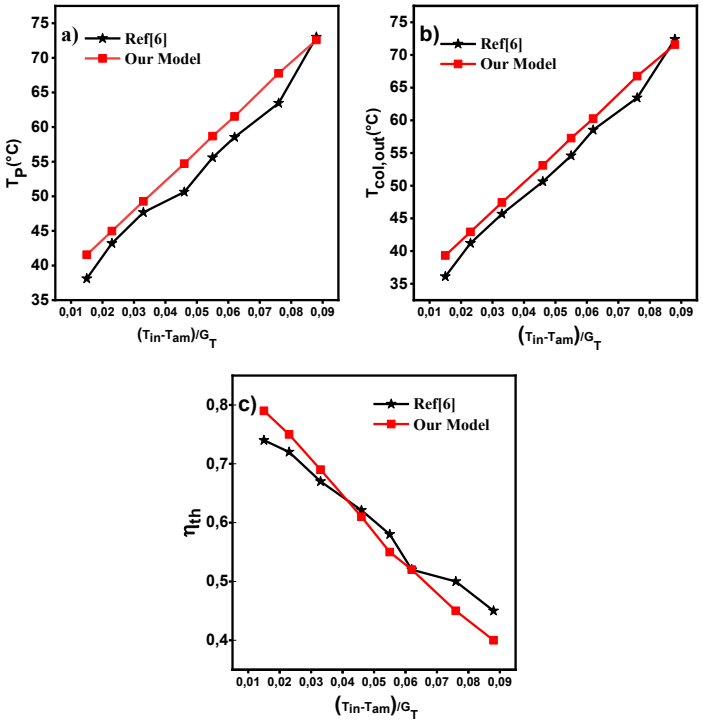


**Fig. 3.** Comparative analysis of FPC test results: Experimental[6] vs. Numerical.

Figures (a–c) depict a comparative analysis between the experimental and numerical results. The numerical model consistently considered important parameters such as mass flow rate, inlet temperature, and solar irradiation. The computed outputs of the numerical model included plate temperature, collector outlet temperature, and thermal efficiency. The numerical results are compared to experimental data obtained under the same operational

conditions. This comparison is shown in Figures (a), (b), and (c), which represent the plate temperature, collector outlet temperature, and thermal efficiency, respectively.

The calculated average errors in these figures, quantifying the disparities between the numerical model's predictions and the experimental data, are found to be 5.28%, 4.48%, and 5.18%, respectively. These values, characterized by their comparably modest magnitudes, affirm the robust reliability of the developed numerical model for the studied FPC tests.

### *3.2.1 Steady state conditions*

The numerical model allows us to analyze and study the influence of different parameters on the performance of the system. To study the influence of a parameter, we vary it from a reference state and keep the other parameters constant. By keeping the temperatures of the external sources constant, we study the influence of the different temperatures in the system: the temperature of the evaporator $T_e$ and the temperature of the condenser $T_c$. The results are presented in the figure 4 (Figs. a and b). We have also studied the influence of the efficiency of the heat exchanger (Fig. c) on the performance of the system.

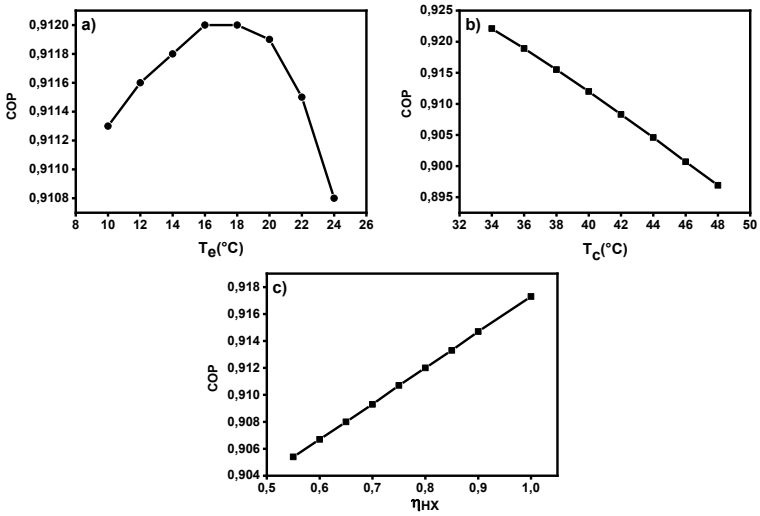


**Fig. 4.** Variation of the coefficient of performance as a function of: a) the evaporator temperature; b) the condenser temperature; c) the heat exchanger efficiency.

The results show that the temperature parameters have a great influence on the performance of the system. It is best to work with an evaporator temperature where the coefficient of performance is at its highest and a lower condenser temperature. Increasing the efficiency of the heat exchanger significantly increases the coefficient of performance. This proves the usefulness of having a heat exchanger in this type of system.

### *3.2.2 Quasi-steady state conditions*

In this section, we study the reliability of such an approach in the real case where $T_{amb}$, $V_w$, and $G_T$ depend on the weather (quasi-static model). Figure 2 shows the weather data of a hot day in August 2021 in the city of Meknès, Morocco.
The goal of this project is to know if a flat plate solar collector could be used to power an air conditioner in very hot conditions while keeping thermal comfort of occupants. For this, we will use a fan. Table 2 shows the characteristics of the fan cooler.
Using equation 24, we can calculate the cooling load to cool $M_{air}$ from 35°C to 18°C, and we find $Load$ = 1.64 kW. Fig. 5 shows that the available solar capacity $Q_u$ supplied by the flat plate collector does not exceed 1.64 kW in a limited time interval, i.e., the flat plate collector is effective in powering a cooling machine with a load of 1.64 kW just for a part time of the day.

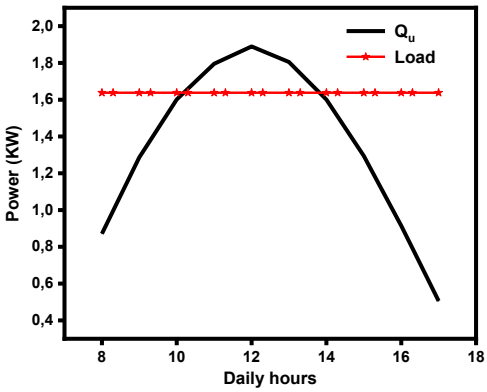


**Fig. 5.** Cooling load and useful solar thermal capacity supplied by the flat plate collector during the examined summer day.

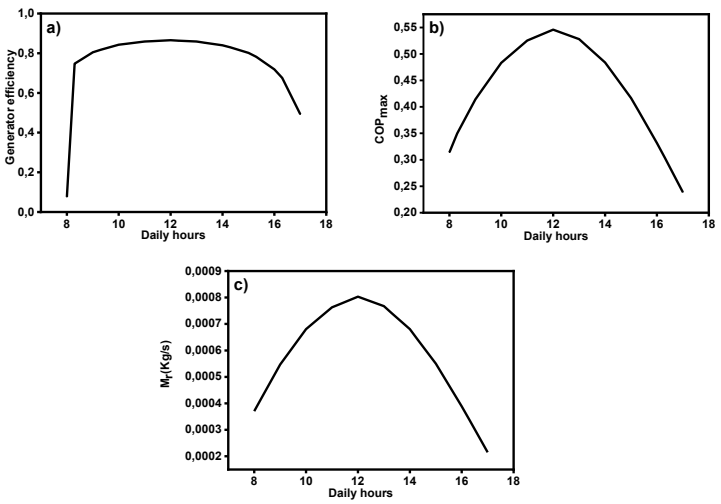


**Fig. 6.** Performance parameters during the examined summer day: a) the generator efficiency; b) the system maximum COP; c) the refrigerant mass flow rate.

Figure 6 offers a comprehensive analysis of the findings from our study, focusing on three crucial indicators of system performance: the efficiency of the generator, the maximum

coefficient of performance (COP), and the rate of refrigerant mass flow observed on the selected summer day under examination. During this specific time frame, there is a notable increase in solar irradiation, resulting in an advantageous period for attaining maximum values in these essential physical parameters.
During the period characterized by high solar irradiation, we observed that the refrigerant mass flow rate reached optimal levels, resulting in improved generator efficiency. As a consequence, this results in a notable increase in the maximum coefficient of performance (COP) of the system. The evident association between solar irradiation and system performance highlights the significance of efficient solar energy management in maximizing the efficiency of refrigeration systems.

## 4 Conclusion

This study examined the impact of condenser and evaporator temperatures, as well as the heat exchanger efficiency, on the overall performance of the system. The results show that the temperature parameters have a significant impact on the system's performance. Optimal performance is achieved by operating with an evaporator temperature that maximizes the coefficient of performance while maintaining a lower condenser temperature. Enhancing the efficiency of the heat exchanger leads to a significant increase in the coefficient of performance.

The investigation is being conducted with a specific emphasis on the optimization of the system. This study carefully looks into whether this method could be used in real-life situations where important variables, like ambient temperature ($T_{am}$), wind speed ($V_w$), and total solar irradiance ($G_T$), change over time in a way that can be explained by a quasi-static model. Our simulation studies have demonstrated that the optimal utilization of a flat-plate solar collector for energizing our system requires specific solar irradiance conditions. The progression of our research is anticipated to be enhanced through a sustained focus on the optimization of the system.

## Nomenclature

| | |
|---|---|
| $A_c$ | *Collector area,* $m^2$ |
| $C_p$ | *Specific heat capacity,* $KJ.Kg^{-1}.K^{-1}$ |
| *COP* | *Coefficient of performance, -* |
| $D_i$ | *Tube inner diameter, m* |
| $D_o$ | *Tube outer diameter, m* |
| *Eff* | *Efficiency, -* |
| $F''$ | *Collector flow factor, -* |
| $F_R$ | *Collector heat removal factor, -* |
| $G_T$ | *Incident solar irradiation,* $W.m^{-2}$ |
| *H* | *Enthalpy,* $KJ/Kg$ |
| *k* | *Thermal conductivity,* $W.m^{-1}K^{-1}$ |
| *L* | *Tube length, m* |
| *Load* | *Cooling load, kW* |
| *M, m* | *Mass flow rate,* $Kg.s^{-1}$ |
| $N_{riser}$ | *Number of risers, -* |
| *Q* | *Heat flux, W* |
| *T* | *Temperature, K* |
| $U_b$ | *Back thermal loss coefficient,* $W.m^{-2}.K^{-1}$ |
| $U_e$ | *Edge thermal loss coefficient,* $W.m^{-2}.K^{-1}$ |
| $U_L$ | *Overall heat loss coefficient,* $W.m^{-2}.K^{-1}$ |
| $V_w$ | *Ambient wind velocity,* $m.s^{-1}$ |
| *W* | *Distance between tubes, m* |
| *X* | *Concentration percentage, %* |

**Greek symbols**

| | |
|---|---|
| $\alpha$ | *Plate absorbance, -* |
| $\beta$ | *Collector slope, °* |
| $\delta$ | *Thickness, m* |
| $\varepsilon$ | *Emittance, -* |
| $\eta$ | *Efficiency, -* |
| $\tau$ | *Cover transmittance, -* |

**Subscripts and superscripts**

| | |
|---|---|
| *a* | *Absorber* |
| *ai* | *Inlet hot air* |
| *air* | *Air* |
| *ao* | *Outlet cooled air* |
| *a,hex* | *From absorber to heat exchanger* |
| *c* | *Condenser* |
| *c,evp* | *From condenser to evaporator* |
| *col* | *Collector* |
| *col,in* | *Collector inlet* |
| *col,out* | *Collector outlet* |
| *e* | *Evaporator* |
| *e,abs* | *From evaporator to absorber* |
| *fm* | *Mean fluid* |
| *g* | *Generator* |
| *g,cond* | *From generator to condenser* |

| | | | |
|---|---|---|---|
| *g,hex* | *From generator to heat exchanger* | *r* | *Refrigerant* |
| *hex,HX* | *Heat exchanger* | *str* | *Strong* |
| *hex,a* | *From heat exchanger to absorber* | *sol* | *Solar* |
| *hex,g* | *From heat exchanger to generator* | *th* | *Thermal* |
| *ma* | *Mean air* | *u* | *Useful* |
| *p* | *Plate* | *wk* | *Weak* |
| *pm* | *Mean plate* | | |

## References

1. Fan, Y., Luo, L., Souyri, B. Renew. Sustain. Energy Rev. 11, 1758–1775 (2007).
2. Duffie, J.A., Beckman, W.A. Solar Engineering of Thermal Processes. John Wiley & Sons INC (1991).
3. Bellos, E., Tzivanidis, C. Therm. Sci. Eng. Prog. 2, 71e79 (2017).
4. H.U. Helvaci, Z.A. Khan. Energy Conversion and Management. Volume 106. Pages 139-150 (2015).
5. Adil Al-Falahi, Falah Alobaid, Bernd Epple. Case Studies in Thermal Engineering. Volume 22, 100763 (2020).
6. Bellos, E., Tzivanidis. J. Clean. Prod. 174, 256-272 (2018).
7. NASA Prediction of Worldwide Energy Resources[https://power.larc.nasa.gov]